

See discussions, stats, and author profiles for this publication at: <https://www.researchgate.net/publication/51721957>

Stability and Robustness of Human Metabolic Phenotypes in Response to Sequential Food Challenges

ARTICLE in JOURNAL OF PROTEOME RESEARCH · FEBRUARY 2012

Impact Factor: 4.25 · DOI: 10.1021/pr2005764 · Source: PubMed

CITATIONS

52

READS

35

7 AUTHORS, INCLUDING:



Silke Heinzmann
Helmholtz Zentrum München

13 PUBLICATIONS 139 CITATIONS

[SEE PROFILE](#)



Claire Alexandra Merrifield
Imperial College London

10 PUBLICATIONS 130 CITATIONS

[SEE PROFILE](#)



Sunil Kochhar
Nestlé S.A.

119 PUBLICATIONS 4,719 CITATIONS

[SEE PROFILE](#)



Jeremy K Nicholson
Imperial College London

740 PUBLICATIONS 43,971 CITATIONS

[SEE PROFILE](#)

Stability and Robustness of Human Metabolic Phenotypes in Response to Sequential Food Challenges

Silke S. Heinzmann,[†] Claire A. Merrifield,[†] Serge Rezzi,[‡] Sunil Kochhar,[‡] John C. Lindon,[†] Elaine Holmes,^{*,†} and Jeremy K. Nicholson^{*,†}

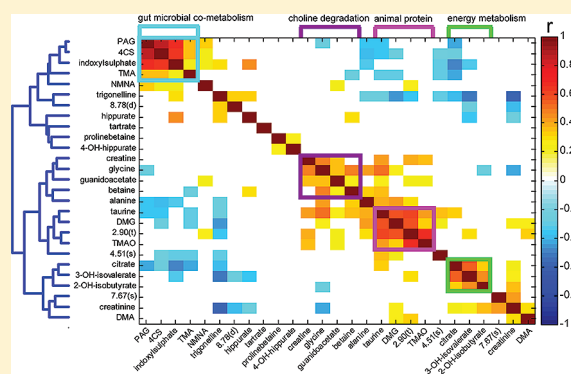
[†]Biomolecular Medicine, Department of Surgery & Cancer, Imperial College London, Sir Alexander Fleming Building, South Kensington, London, SW7 2AZ, United Kingdom

[‡]Nestle Research Center, Vers-chez-les-Blancs, CH-1000 Lausanne 26, Switzerland

Supporting Information

ABSTRACT: High-resolution spectroscopic profiles of biofluids can define metabolic phenotypes, providing a window onto the impact of diet on health to reflect gene–environment interactions. ¹H NMR spectroscopic profiling was used to characterize the effect of nutritional intervention on the stability of the metabolic phenotype of 7 individuals following a controlled 7 day dietary protocol. Inter-individual metabolic differences influenced proportionally more of the spectrum than dietary modulation, with certain individuals displaying a greater stability of metabolic phenotypes than others. Correlation structures between urinary metabolites were identified and used to map inter-individual pathway differences. Choline degradation was the pathway most affected by the individual, suggesting that the gut microbiota influence host metabolic phenotypes. This influence was further emphasized by the highly correlated excretion of the microbial–mammalian co-metabolites phenylacetylglutamine, 4-cresylsulfate ($r = 0.87$), and indoxylsulfate ($r = 0.67$) across all individuals. Above the background of inter-individual differences, clear biochemical effects of single type dietary interventions, animal protein, fruit and wine intake, were observed; for example, the spectral variance introduced by fruit ingestion was attributed to the metabolites tartrate, proline betaine, hippurate, and 4-hydroxyhippurate. This differential metabolic baseline and response to selected dietary challenges highlights the importance of understanding individual differences in metabolism and provides a rationale for evaluating dietary interventions and stratification of individuals with respect to guiding nutrition and health programmes.

KEYWORDS: Human, Metabolic Phenotype, NMR spectroscopy, Metabolic Profiling, Urine, Microbiota, Diet, Pattern recognition, Phenylacetylglutamine, 4-Cresylsulphate



INTRODUCTION

A major objective of 21st century nutritional research is the generation of personalized lifestyle recommendations to improve health and quality of life based on knowledge of the biology of the individual. Metabolic phenotypes or metabotypes¹ each provide metrics of gene–diet–environment–microbiome interactions and are statistically and biologically related to disease risk factors.^{2,3} It is therefore important to characterize the metabolic phenotype of individuals and to establish the extent to which we can influence their baseline phenotype by nutritional and lifestyle interventions. The nutritional status embodies much more than the balance between nutrient intake and energy expenditure, since appropriate nutritional intake can prevent disease development and promote overall well-being and healthy aging.^{4,5}

Measuring changes in multiple metabolite concentrations is a powerful approach for assessing the nutritional status of humans and can be integrated with anthropometric and behavioral measurements, to help estimate an individual's nutritional phenotype.⁶ Metabolic profiles generated using high resolution analytical tools such as nuclear magnetic resonance (NMR) spectroscopy

and liquid chromatography–mass spectrometry (LC–MS) can be mined using mathematical modeling methods,⁷ and these together provide a powerful platform for characterizing the metabolic phenotype of a person based on the composition of their biofluids and tissues. In recent years, a number of metabolic profiling studies have been undertaken to assess the metabolic phenotype of healthy humans. Efforts have also been directed toward describing metabolic differences between subjects on the basis of age, gender and BMI,⁸ culture and diet preferences,^{9,10} menstrual cycle,¹¹ and diurnal variation¹² and as such have focused on the individual metabolic phenotype as a starting point for lifestyle intervention. Distinguishing urinary metabolite profiles between individuals have previously been described,¹³ where multiple urinary samples from 22 individuals were correctly predicted to the donors in a supervised pattern recognition approach. Extending the analysis to sample collections across 3 years revealed a set of 12 metabolites that consistently allowed

Received: June 14, 2011

Published: October 17, 2011

the identification of these individuals.¹⁴ However, dietary studies have mainly focused on the effects of dietary interventions on the metabolic phenotype without specific consideration of interindividual differences in basal metabolic profiles or their day-to-day stability.^{10,15–18} All humans have some unique genetic and lifestyle features that impact on the metabotype and its variability, and a key question is whether this metabolic starting point is predictive of the outcome of a drug or lifestyle intervention.² Clayton et al. described the proof-of-principle of such a prediction strategy, the pharmaco-metabonomics concept, for drug toxicity in the rat¹⁹ and drug metabolism in man.²⁰ They showed the feasibility of predicting acetaminophen metabolism and excretion based on the metabolic profile of a predose urine sample, and a further study in man showed potential for predicting early acetaminophen-related hepatotoxicity.²¹ These proof-of-principle studies lend credence to the broad possibility of being able to stratify individuals with respect to optimizing their nutrition.

This manuscript reports the results from a short-term diet-controlled study investigating the contribution of metabolic baseline differences in healthy individuals using various multivariate statistical techniques to analyze and stratify urinary profiles under various dietary modulations. Several metabolic pathways are described that are heavily influenced by inherent individual differences and contrasted with metabolites that were relatively consistent between individuals. The effect of various dietary components (“diet challenges”) including animal protein, fruit and wine/grapes were assessed in terms of the added metabolic variation they introduced against the variation attributed to inter-individual differences. This study helps to better define a “standard” metabolic phenotype and elucidate how modification of diet may impact upon the metabolic profile with the aim of understanding and maintaining a healthy metabolic profile and its stability to dietary influences.

MATERIAL AND METHODS

Nutrition Study Data Set

To investigate the influence of food consumption on the metabolic phenotype of urine, a nutritional intervention study was undertaken. The food challenge study presented herein involved the recruitment of 7 volunteers (6 females (volunteers 1–5 and volunteer 7), 1 male (volunteer 6), 28–45 years) that met the inclusion criteria; healthy, aged 18–45 years, nonsmoker and BMI 18–25 kg/m² and absence of regular drug intake and regular food supplements and no antibiotic use within the last 3 months. Participating women were asked to conduct the study in the first week after their monthly period. Participants consumed a standardized breakfast, lunch and dinner, comprised of whole-grain bread and cheese (breakfast), ham sandwich (lunch) and pasta with tomato sauce (dinner) from the run-in day (day 0) until lunch on day 3. Water and one cup of coffee/tea daily were allowed as beverages. In addition to the standard dinner, supplementary meals were introduced: mixed fruit (apple, orange, grapes and grapefruit) on the evening of day 2, fish on day 3, wine and grapes on day 4, beef on day 5 and a fish lunch on day 6. To ensure a high degree of compliance to the food consumption regime and to check for its accuracy, all participants kept a food diary over the whole course of the study, where time of consumption and composition of the consumed foods were noted. Furthermore, close personal contact was kept on a daily basis with all participants. Urine was collected 4 times per day (first morning urine, before lunch, before dinner and at bed time), from the

morning of day 1 until the morning of day 7. Urine specimens were collected into sterile tubes (Sterilin, U.K.) and stored at –40 °C until analysis.

¹H NMR Spectroscopic Analysis of Urine Samples

¹H NMR spectra were acquired on a Bruker Avance 600 MHz spectrometer (Bruker Biospin, Rheinstetten, Germany) operating at 600.13 MHz. A standard 1-dimensional (1D) pulse sequence [recycle delay (RD)-90°-t1-90°-tm-90°-acquire] free induction decay (FID) was used with water suppression irradiation during RD of 2 s, and the mixing time (tm) set to 100 ms, the 90° pulse width was 10 μs. Spectra were acquired by collecting 128 scans into 32 K data points with a spectral width of 12000 Hz. For spectral processing, FIDs were multiplied by an exponential function corresponding to a line broadening of 0.3 Hz before Fourier transformation. All spectra were manually phased, baseline corrected and referenced to TSP (δ 0.0) and exported into Matlab (2009a, The Mathworks Inc., MA) for data analysis. The spectra were aligned using a recursive segment-wise peak alignment algorithm²² and normalized using a probabilistic quotient normalization algorithm²³ to partially account for urinary dilution effects.

Multivariate Statistical Analysis of the Urinary Metabolite Profiles

All timed spot urine specimens that were collected on day 1 in the morning until evening of day 2 (before fruit meal) were defined as “standard class”; specimens collected up to 24 h after the fruit meal (bed time of day 2 until evening of day 3) were defined as “fruit class”, up to 24 h after fish (bed time of day 3 until evening of day 4 and afternoon day 6 until morning day 7) and beef (bed time day 5 until lunch day 6) to “animal protein class”, up to 24 h after wine and grapes (bed time of day 4 until evening of day 5) to “wine class”. Spectra were also analyzed using each participant as a classifier, regardless of dietary intervention.

Three types of unsupervised algorithms were compared to ascertain the inherent metabolic variation across participants: principal component analysis (PCA), hierarchical cluster analysis (HCA) and self-organizing mapping (SOM).

Principal Component Analysis (PCA). PCA was conducted in Matlab on the whole data set and the number of components was selected on the basis of the cumulative value for the R² (explained variance) and Q² (predictive ability) parameters such that components were included if R² was maintained or increased with a corresponding Q² increase of >2%.

Hierarchical Cluster Analysis (HCA). HCA was carried out using the Matlab Statistical Toolbox; the same data set was used as for PCA analysis (e.g., full resolution spectral data, including all volunteers). Sample distance was measured using Euclidian distance and linkage analysis was achieved by calculating the average distance. A dendrogram showing the similarity and distance of each sample in the data set was plotted, and data tree branches color-coded for sample donor (volunteer). A second “identically” structured dendrogram was coded according to dietary intervention.

Self Organizing Maps (SOM). The SOM algorithm was implemented using the SOM Toolbox 2.0 (<http://www.cis.hut.fi/projects/somtoolbox>). The resolution of the data set was reduced to δ 0.01 for better data handling (e.g., faster model calculation). This algorithm randomly assigns node weight vectors in the map and calculates the Euclidean distance (batch training) between the node vector and the input (sample) vector and drops the sample into the node with the smallest distance between sample vector and node vector. This is an iterative process and the node is constantly updated via a Gaussian neighborhood

function. Each sample is then plotted onto the node map and color-coded for (i) sample donor and (ii) food challenge.

Calculation of Variable Stability. In order to assess the relative stability of metabolic variation, a partial least squares discriminant analysis (PLS-DA) was carried out on spectral bins (bin width δ 0.01) using 7-fold cross validation. Two models were calculated: food-related differences (4 food classes: standard, fruit supplement, animal protein supplement, wine and grape supplement) were elucidated using 3 predictive components and inter-individual differences (7 volunteers) were calculated into 6 predictive components. An output figure was created plotting the model parameters R^2Y (goodness of fit) and Q^2Y (predictive ability) superimposed upon a mean spectrum to identify spectral areas of good modeling and predictivity with respect to predicting either dietary response or inter-individual differences.

Variance Components Analysis. A variance components model was calculated to show the relative contribution of each of the food challenges to the variance of each data point in the NMR spectrum. This approach uses a 2^3 full factorial design as the Y matrix and the NMR spectral information as the X matrix.²⁴

Characterization of Inter-individual Differences in Metabolic Phenotype. Pair-wise orthogonal partial least-squares discriminant analysis (OPLS-DA)²⁵ was carried out in Matlab, comparing urine samples obtained from each volunteer to all other volunteers. The sample donor was used as the "Y" variable whereby a selected donor was designated as class 1 and all other participants were combined to form a second composite class. All resonances with a correlation coefficient greater than 0.2 (selected as a heuristic cutoff) were tabulated.

Investigation of Individual Metabolite Excretion Kinetics

To compare the relative amount of urinary metabolite excretion associated with different food challenges and different volunteers, several peaks of each NMR spectrum, chosen from the inter-individual and differential food challenge model coefficients, were integrated using Matlab and plotted against sampling time. Thus, the presence of certain metabolites and their subsequent increased or decreased excretion were monitored over time in response to dietary and/or temporal changes. Participant 1 repeated the diet 3 months after the first study to assess the reproducibility of the dietary responses.

■ RESULTS AND DISCUSSION

Mapping the Inherent Variation in Urinary Metabolite Profiles under Different Dietary Conditions

Urinary metabolic phenotypes were characterized for all 7 volunteers (up to 25 timed samples per person) using three different unsupervised multivariate statistical methods, HCA, SOM and PCA. The three types of analysis were broadly consistent and showed that (i) each volunteer tended to occupy their own metabolic space (Figure 1A,C and SI Figure 1A,B, Supporting Information) and (ii) of the three short-term dietary interventions (fruit, wine, animal protein), only animal protein consumption introduced systematic metabolic changes strong enough to move each person's metabolic profile to a new, shared metabolic space (Figure 1B,D and SI Figure 1C,D, Supporting Information). Hierarchical cluster analysis was performed, which provides a measure of the closeness of groups. The input data are summarized into a dendrogram where the branch lengths reflect the differences among the groups and thus this method provides

an easy visualization of the similarities of samples. Different distance measures, such as Euclidean distance or distance based on correlation can be applied. Clustering trends due to inter-individual differences were apparent across the HCA dendrogram (Figure 1A), whereas food influences were only visible for the animal protein challenge (Figure 1B). Within this interindividual variance dominated pattern, certain individuals were found to have a more consistent metabolic profile than others, regardless of dietary changes. For example, it was apparent that participants 1, 3, 5, and 6 had more homogeneous urinary metabolite profiles than the other participants whereas participant 7 showed a particularly diverse metabolic composition with samples dispersed throughout the map. Since supervised pattern recognition analysis maximizes class separation for enhanced biomarker recovery, identification of key discriminatory metabolites for each volunteer was performed in a separate supervised analysis. An orthogonal statistical procedure, self-organizing maps, was also conducted. Self-organizing maps are, like HCA, unsupervised, but use an artificial neural network to visualize complex data onto a 2D plane of nodes. It has apparent advantages when attempting to visualize and relate nonlinear, complicated data sets^{26,27} and is not susceptible to outliers. SOMs are a type of artificial neural network that map observations based on their relative similarity to each other in an unsupervised, nonlinear fashion. Here, each sample is represented by a pie section in a node and color-coded for either the sample donor (Figure 1C) or food consumption (Figure 1D). The SOMs allow an additional piece of information to be encoded in the maps such that in addition to the individual sample, the whole node can be color-coded for an individual/food challenge if the majority of the sections in the node are from the same donor or food class, respectively. The SOM plots show a similar picture but here the variation in the profiles introduced by consumption of animal protein is clearer to detect at a superficial level (Figure 1D). As with HCA, the SOM plots showed that participants 1, 3, and 6 were distinct from the other participants. However, although the consensus from HCA and SOM models was good, each of these methods offered a degree of independent information. For example, samples from participant 5 were clustered in the HCA plot but were dispersed through the SOM plots, whereas participant 2 showed more homogeneous metabolite profiles across the SOM nodes than was apparent from the HCA dendrogram. The only male volunteer (volunteer 6) did not introduce distinct gender-based separation and since only 1 male volunteer was included in the study, it was not possible to investigate metabolite differences based on gender.

In a third analysis, PCA was conducted (SI Figure 1, Supporting Information), as this is the most commonly applied unsupervised algorithm to metabolic profiling data, and the scores plots show clustering trends due to inter-individual differences in each of the first six principal components. Food influences were visible in principal component 4, but not the lower components. PCA was subsequently performed on the samples from the standard diet class only, in order to exclude food-related differences and focus on inter-individual variation, and showed improved separation of participants indicating the benefit of aligning diets prior to commencing nutritional interventions (SI Figure 2, Supporting Information). PCA assumes that n -dimensional data can be reduced to linear combinations of the data ("principal components"). Furthermore, PCA is susceptible to outliers, that is, the leverage effect of outliers can disturb the projection.

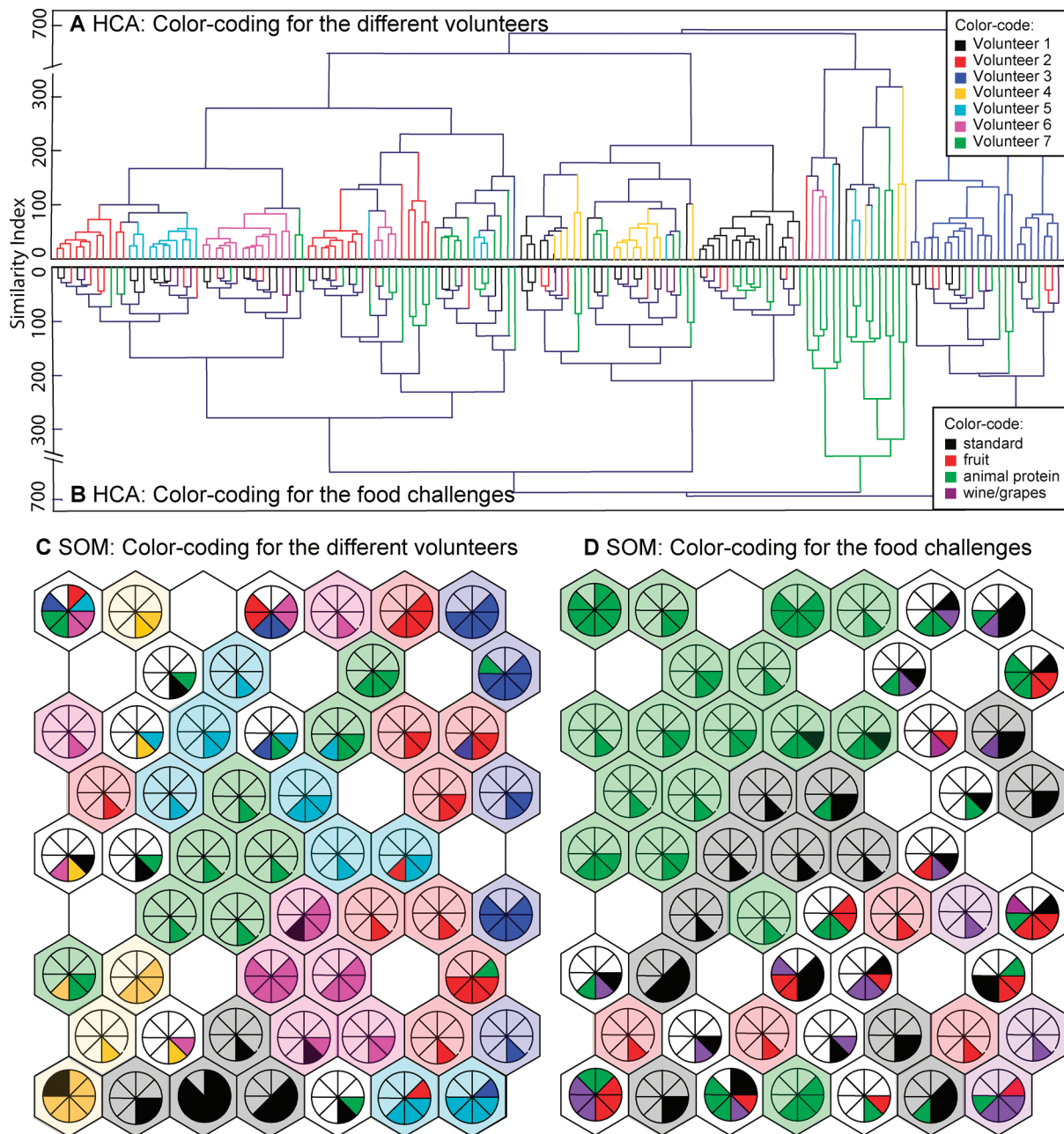


Figure 1. (A,B) Hierarchical clustering analysis dendrogram (Euclidean distance, Ward linkage) derived from the ¹H NMR spectral data. The same dendrogram is presented twice with each sample (=dendrogram branch) color coded for (A) the donor of the urine sample and (B) food challenge. (C,D) Self-organizing map of the ¹H spectral data. The map was created as described in the methods and color-coding superimposed for (C) volunteer, that is, urine sample donor and (D) food challenge, that is, sample collected in the 24-h time frame after this food consumption. Whole nodes were highlighted according to volunteer or food color, if a majority of nodes belonged to the same class. Both analyses were color-coded by individuals and by food groups.

If many principal components are needed to capture the majority of relevant variation, the visualization power is reduced as information is distributed across many components.

Although the three modeling methods gave broadly similar results, emphasizing the strong influence of inter-individual variability, each method provided subtle differences in the extraction of information. Of the three modeling methods used, HCA gave the best summary of information in a single dimension, whereas 4 dimensions were necessary to adequately describe dietary variation in the PCA models. However, the loadings or

variable contributions are easier to extract from the PCA models, and therefore easier to interpret than HCA. Additionally, the use of a single dimension can be a drawback, as it does not allow the possibility to disperse variation into an *n*-dimensional space of principal components.

Thus, regardless of dietary patterns, each individual has a core metabolic fingerprint, influenced by a combination of many factors such as host metabolism, gut microbiota composition, dietary habits, physical activity, and body composition. The findings presented here are consistent with previous studies

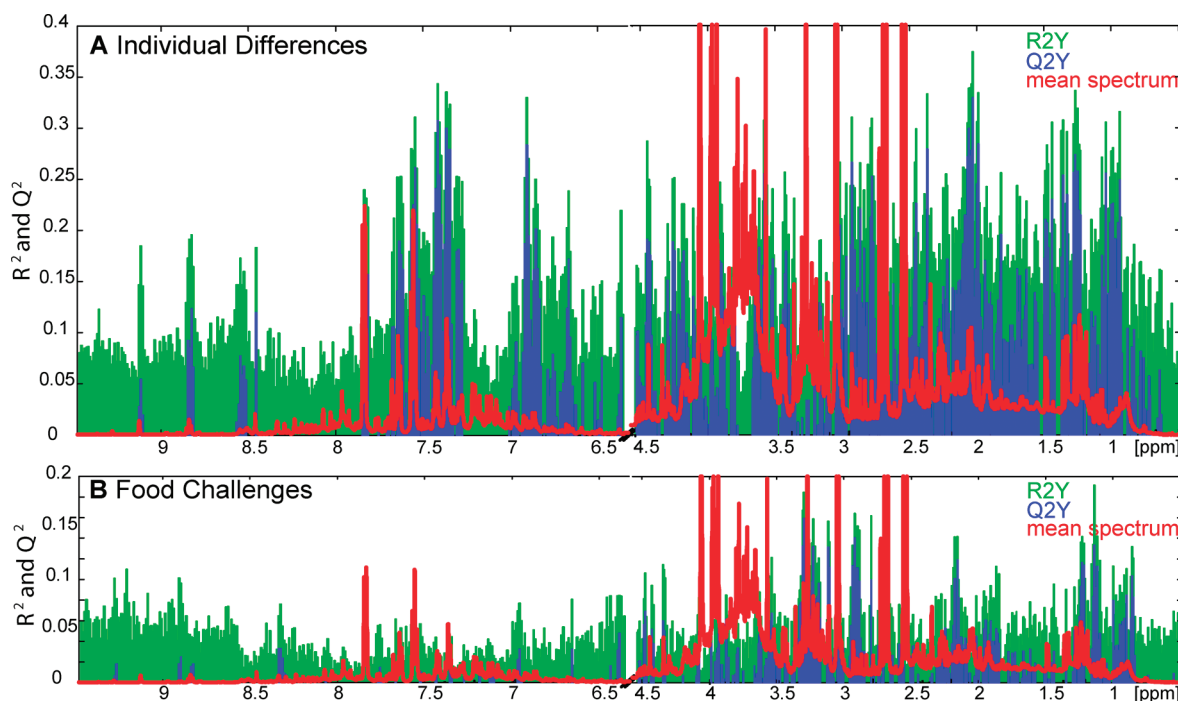


Figure 2. PLS-DA model for (A) individual (6 components) and (B) food challenges (3 components) to highlight information-dense (positive Q^2Y) and nonpredictive (low or negative Q^2Y) spectral areas. Positive values for R^2Y and Q^2Y are shown for each spectral block in green and blue respectively. Metabolic changes related to food challenges were sparse and only a few defined spectral regions were predictive of food challenges, while inter-individual differences were found across the whole spectrum, especially in the aromatic proton area (δ 6.5–8).

demonstrating inter- and intra-individual variation: that reported inter-individual differences are greater than intraindividual differences with the greatest variation in the first morning urine sample.^{18,28} Assfalg et al.¹³ and Bernini et al.¹⁴ have also described personal metabolic phenotypes using a series of supervised pattern recognition techniques. Although this study included only a limited number of volunteers, the findings have implications for future intervention studies, suggesting that nutritional standardization is not necessary, as long as food sources introducing strong metabolic changes, such as extreme intake of animal protein, are excluded.

Stability and Robustness of Variables in Relation to Individual Metabotype and Diet

To establish which spectral regions carry robust information to distinguish food-related and inter-individual differences, PLS-DA analysis was carried out on spectral blocks (block width δ 0.01) and the model parameters R^2Y and Q^2Y were plotted, along with a superimposed mean NMR urine spectrum (Figure 2). Metabolites that robustly described inter-individual differences permeated most of the spectrum, in the areas δ = 0.7–8, and selected areas between δ = 8.4 and 9.2 (Figure 2A). Conversely, spectral regions that were predictive of food-introduced metabolic differences were fewer in number and lower in predictive strength (Q^2Y) in general. Food consumption introduced metabolic differences in defined areas such as δ = 0.85–1.35, δ = 1.9–2.3, δ = 2.8–3.6 and δ = 4.3–4.5 (Figure 2B). Interestingly, the spectral areas containing aromatic chemical structures (δ = 6.5–9.5) are often descriptive of gut microbial activity, and were more predictive of inter-individual rather than food-related changes. Further investigation involving relative quantification of gut microbial co-metabolism

is described later. As expected, signal-poor areas (e.g., δ < 0.5 and > 9.5) were not predictive in either model. The data set was broken down into subsets describing pairwise comparisons of dietary classes involving comparison of fruit, wine and animal protein samples with the standard diet class, using variance components analysis. Focusing on single dietary challenges improved the predictivity of several spectral regions and identified metabolites associated with each dietary challenge (Figure 3A,B). This analysis was used as a filter to improve food-related differentiation. The 20 spectral regions corresponding to the highest Q^2 values in each of the three food comparisons were combined and PCA repeated on the reduced subset to better differentiate the samples according to food class (Figure 3C,D). These regions (10.2% of total spectral area) contained 3-methylhistidine, trimethylamine-N-oxide (TMAO), (phospho-) choline, taurine and carnitine, which were associated with consumption of animal protein; proline betaine,²⁹ 4-hydroxyhippurate and fruit acids associated with the fruit class; and ethanol, tartrate and wine acids /-diols (e.g., 2-isopropylmalate, diethylmalonate, 2,3-butanediol) associated with wine consumption. A PCA analysis based on the selected 20 spectral regions confirms strong separation of urine samples collected after each specific food intake. This approach also identified 2 outlying samples in PC 3 (Figure 3D), where a volunteer under fish meal challenge deviated from the food protocol and also consumed an orange. Thus the use of “biomarker windows” can facilitate enhanced classification according to nutritional intervention above the background structure of inter-individual metabolic phenotypes. We have validated this concept for proline betaine as a biomarker for citrus fruit intake previously, based on an international population study,³⁰ and several of the potential animal protein biomarkers have been confirmed by other groups.¹⁶

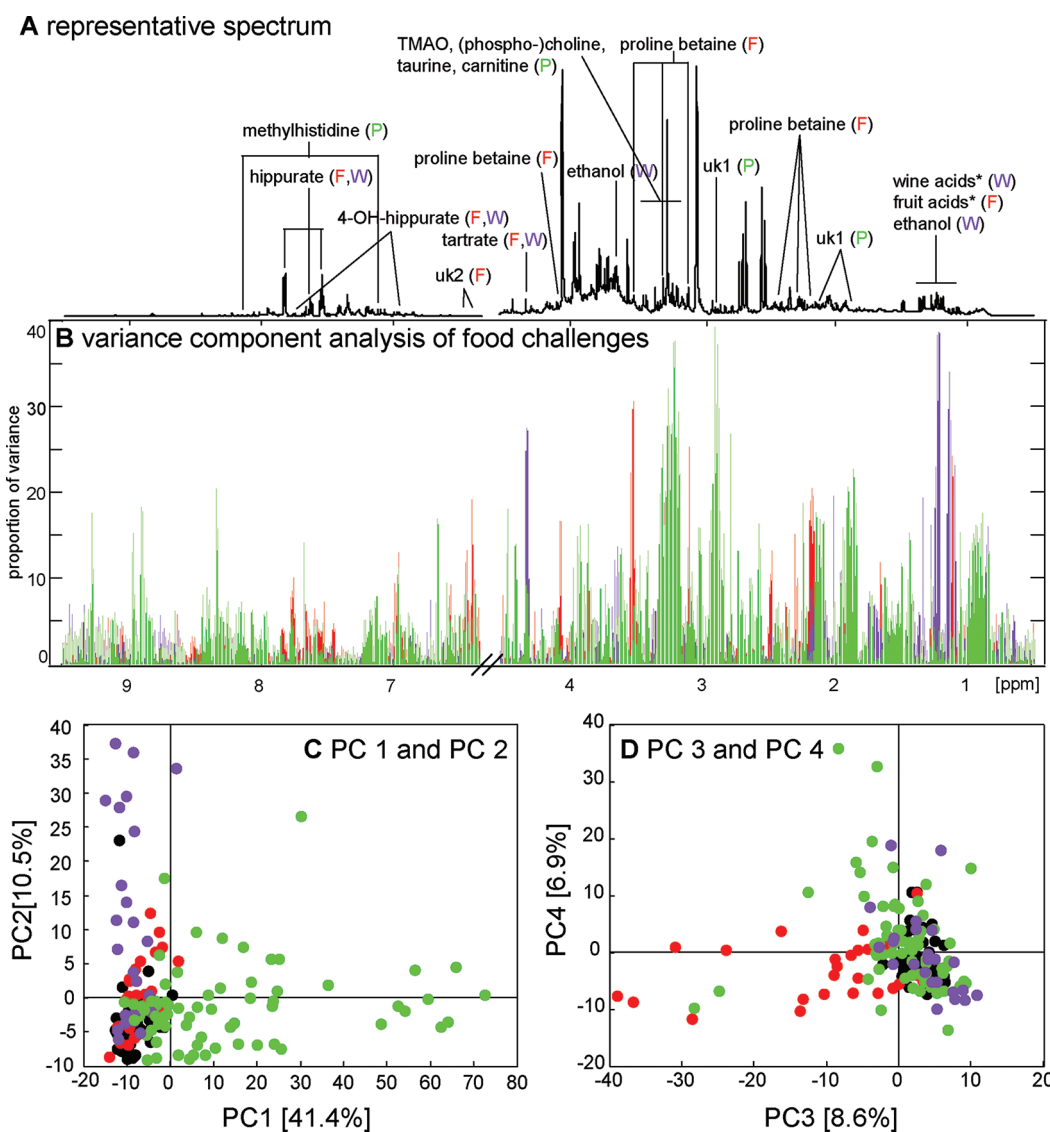


Figure 3. (A) Representative NMR spectrum with potential food biomarkers labeled, using the color-code of the food challenges (fruit (F, red), animal protein (P, green) and wine/grapes (W, purple)). (B) Variance component analysis of the 3 food challenges fruit, animal protein and wine/grapes highlighting the spectral contribution of each food challenge. Abbreviations: wine acids*: 2-isopropylmalate, diethylmalonate, 2,3-butanediol, unknown (δ 1.10 (d), 3.90 (m)); fruit acids*: unknown (δ 1.12 (m)), unknown (δ 1.28 (s)); uk1 (unknown 1): δ 2.13 (dd), 2.57 (m), 2.90 (t), 3.25 (dd), 4.43 (dd); uk2 (unknown 2), δ 6.40 (m), 6.44 (m). (C,D) PCA scores plot from data selected by the 20 spectral regions corresponding to the highest Q^2 values in each of the three food comparisons in Figure 2. This approach also identified 2 outlying samples in PC3, where a volunteer under fish meal challenge deviated from the food protocol and also consumed an orange.

The inclusion of more dietary variation across a larger population is likely to result in larger and/or additional biomarker windows. In conclusion, spectral information of inter-individual differences could be found across the majority of the NMR profile, whereas food-related differences were only described by a few distinct metabolites.

Identification of Metabolites Associated with Individual Metabotype Variation

A supervised pattern recognition approach was carried out to elucidate a set of metabolites for each person, which was descriptive of each volunteer. For this approach, O-PLS-DA analysis was performed, where each volunteer was compared to the composite of all other participants. This resulted in 7 independent O-PLS-DA models, from which the scores plots are shown in

Figure 4. The model parameters from every model revealed good fit ($R^2Y = 74.7\%-92.6\%$) and good predictive ability ($Q^2Y = 59.6\%-85.8\%$) describing the inter-individual variation. The high Q^2 -value suggests a statistical significance, again reinforcing the strong contribution of the individual to the metabolic phenotype. All resonances with a correlation coefficient of greater than 0.2 were selected for discussion. (Based on small group size as a heuristic cutoff after visual inspection. Orientation at $n = 25$ samples and $p < 0.01$, correlation coefficient is 0.15. For future analysis including larger data sets standards published by Chadeau-Hyam et al. will be used.³¹ Some of the metabolite resonances known to discriminate samples in the models were related to minor breaches of the dietary protocol, for example, use of chewing gum (attributed to the detection of mannitol in volunteer 1b) and consumption of tea instead of coffee

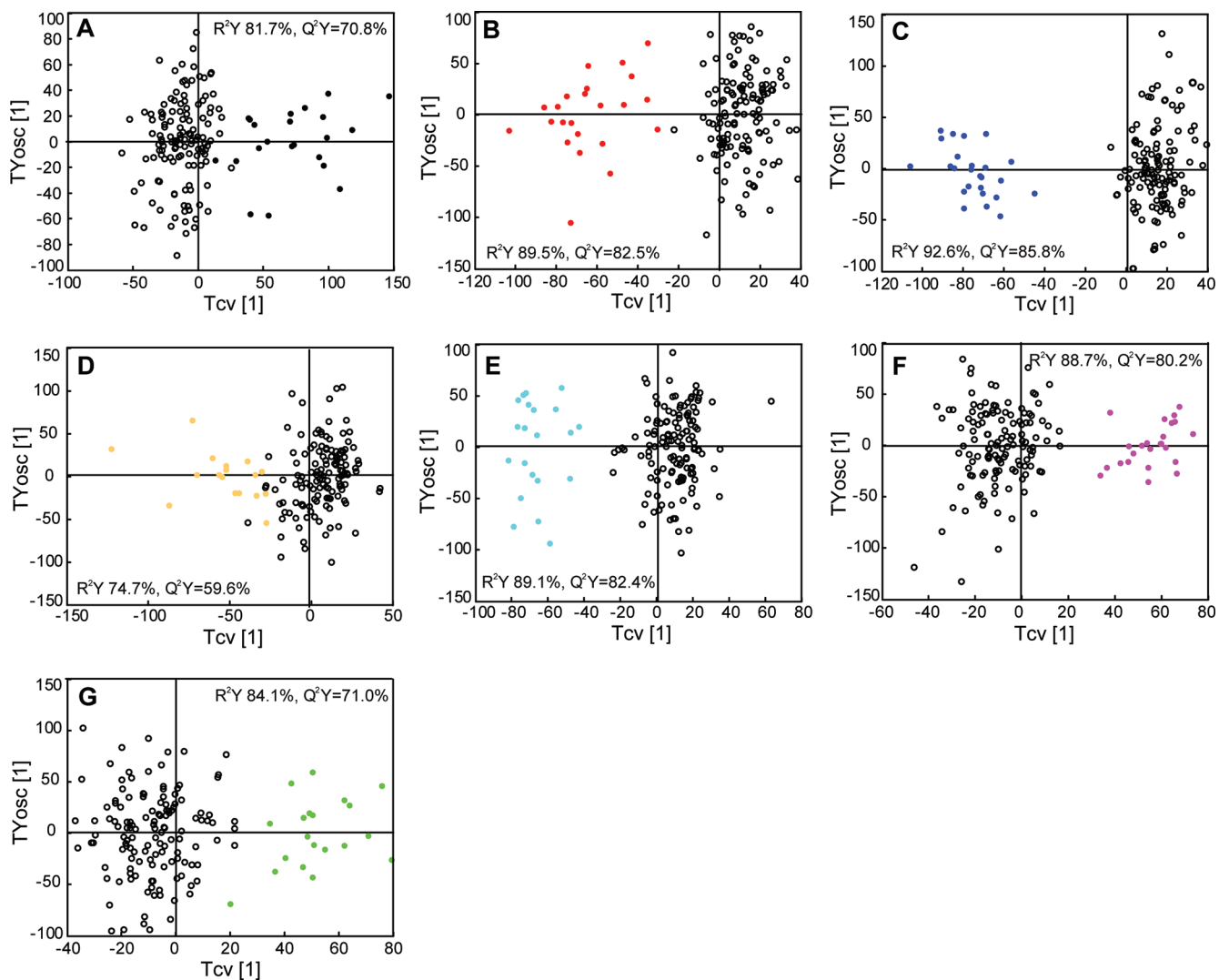


Figure 4. O-PLS-DA scores plots from models using all urine samples, where each individual was compared with the remaining spectra constituting a composite of the other 6 study participants. Each of the 7 models were calculated with 1 predictive and 1 orthogonal component, and the cross-validated (Tcv) and orthogonal (TYosc) scores were plotted. Model goodness (R^2Y) and predictive ability (Q^2Y) are given for each model. Color-code: (A) volunteer 1 (black), (B) volunteer 2 (red), (C) volunteer 3 (blue), (D) volunteer 4 (yellow), (E) volunteer 5 (cyan), (F) volunteer 6 (magenta) and (G) volunteer 7 (green). Open circles: all other volunteers, for each model.

(unknown metabolite with resonances at δ 4.51 (singlet), 6.98 (doublet), 7.38 (triplet) in volunteer 2). Additionally, a few inter-individual differences in responses to food were observed, such as a lack of elevated taurine excretion after animal protein by volunteer 1 and higher excretion of an unassigned compound with chemical shifts at δ 2.90 (triplet), 2.13 (multiplet), 2.57 (multiplet) and 4.43 (doublet of doublets) after fish and beef consumption from volunteer 6. A nontargeted metabolite food analysis could in future help identify unassigned metabolites and guide the origin of these compounds.³⁰ While some urinary metabolites were present in relatively similar concentration across individuals, other metabolites showed a high degree of inter-individual variation. For example, volunteer 3 excreted high creatinine levels in comparison to other participants, volunteer 4 produced high levels of urinary glycine, and volunteer 5 samples were characterized by low hippurate levels. A summary of metabolites differentiating each individual is provided in Table 1.

Effects of Dietary Intervention on Urinary Metabolite Correlation Structures

To gain a better understanding of the relationship between metabolites and how these relationships are affected by dietary changes, representative resonances were relatively quantified by peak integration and a correlation map constructed based on Pearson correlation (Figure 5). This map employed a hierarchical clustering method, using linear correlation to calculate the distance and average distance to create the cluster tree combined with a heat map showing all correlation coefficients (with $p < 0.0019$, for Bonferroni-corrected p -value 0.05).

Strong clustering and correlation was observed between gut microbial or gut microbial-mammalian co-metabolites from protein putrefaction (4-cresylsulphate (4CS), phenylacetylglutamine (PAG) and indoxylsulphate (IS)) and also for metabolites related to protein consumption and choline breakdown (taurine, alanine, dimethylglycine (DMG), TMAO, guanidoacetate, dimethylamine (DMA), glycine, creatine, betaine). Metabolites excreted after

Table 1. Summary of Inter-individual Differences between 7 Volunteers, As Revealed by 7 Independent O-PLS-DA Analyses^a

	metabolite	chemical shift	multiplicity	assignment	r ^b	r ²
Volunteer 1	TMA	2.86	s	CH ₃	↑	0.66
	glutamine	2.45	m	γCH ₂	↓	0.39
	phenylacetylglutamine	7.35	t	H3,H5	↑	0.37
	p-cresyl-sulfate	2.35	s	CH ₃	↑	0.35
	citrate	2.54	d	CH ₂	↓	0.34
	mannitol	3.84	dd	CH ₂ OH	↑	0.29
	N-acetylated metabolite	2.02	s	CH ₃	↓	0.27
	indoxylsulphate	7.50	d	H7	↑	0.23
	DMA	2.77	s	CH ₃	↓	0.23
	N-methylnicotinamide	8.97	m	H6	↑	0.21
	taurine	3.42	t	CH ₂ NH ₂	↓	0.2
	trigonelline	8.84	t	H2	↑	0.18
Volunteer 2	creatinine	4.05	s	CH ₂	↑	0.52
	2-hydroxy-isobutyrate	1.36	s	CH ₃	↓	0.36
	glutamine	2.45	m	γCH ₂	↑	0.22
Volunteer 2	citrate	2.54	d	CH ₂ (ii)	↑	0.64
	creatinine	4.05	s	CH ₂	↑	0.62
	DMA	2.72	s	CH ₃	↑	0.43
	alanine	1.48	d	CH ₃	↑	0.35
Volunteer 4	glycine	3.57	s	CH	↑	0.55
	hippurate	7.55	m	H4	↑	0.3
	trigonelline	9.12	s	CH ₂	↑	0.28
	N-acetylated metabolite	2.03	s	CH ₃	↑	0.28
	creatinine	3.93	s	CH ₂	↑	0.21
Volunteer 5 ^c	3-hydroxy-isovalerate	1.27	s	CH ₃	↑	0.35
	hippurate	7.55	m	H4	↑	0.22
	formate	8.45	s	CH	↑	0.2
Volunteer 6 ^c	glutamine	2.14	m	βCH ₂	↑	0.33
	2-hydroxy-isobutyrate	1.36	s	CH ₃	↓	0.3
	DMG	2.93	s	CH ₃	↑	0.28
	alanine	1.48	d	CH ₃	↑	0.27
	citrate	2.54	d	CH ₂ (ii)	↑	0.25
Volunteer 7	2-hydroxy-isobutyrate	1.36	s	CH ₃	↑	0.3
	N-acetylated metabolite	2.05	s	CH ₃	↑	0.21

^a Each independent analysis compared 1 volunteer vs all other volunteers. Abbreviations: s, singlet, d, doublet, t, triplet, m, multiplet, dd, doublet of doublets. Only resonances assigned to a known metabolite are shown here. ^b Direction of change, (↑) indicates a relatively higher metabolite concentration in this person, (↓) indicates a relatively lower concentration. ^c Several unassigned aromatic resonances.

fruit consumption (hippurate, proline betaine, tartrate, 4-hydroxyhippurate) were mapped adjacently but were not statistically correlated. This might partly be due to the way the fruit was provided in the meal, that is, grapes (containing tartrate) were consumed within the fruit and the grapes/wine challenge, while citrus fruit (containing proline betaine) were only consumed as part of the fruit meal. Furthermore, the excretion kinetics of metabolically inert compounds such as tartrate and proline betaine were different to hippurate and 4-hydroxyhippurate, as the latter two are produced by microbial fermentation of polyphenols.⁵² While hippurate is a metabolite commonly present in the urinary profile, 4-hydroxyhippurate appeared only after fruit consumption. Other metabolite clustering could be observed for metabolites involved in energy metabolism/kidney function (citrate, 2-hydroxyisobutyrate, 3-hydroxyisovalerate) and anticorrelation between some of the gut microbial metabolites (PAG, 4CS) and alanine, taurine, citrate and 3-hydroxyisovalerate (Figure 5) were also shown.

Alteration of Metabolites of Protein Putrefaction/Gut Microbial Co-metabolites

To investigate differences in metabolites related to protein putrefaction by gut microbiota in more depth, the relative concentration of 4CS, PAG and IS were assessed by plotting the peak integrals and their ratios of representative NMR resonances. PAG and 4CS showed the strongest correlation with a correlation coefficient (*r*) of 0.87 (Figure 6A). The correlation coefficients between PAG: IS and 4CS: IS were lower (*r* = 0.67 and 0.63, respectively). The correlation of these three gut microbial metabolites suggests a common dietary source and/or metabolism. It is well established, that the gut microbiota is involved in the anaerobic formation of these compounds from tyrosine, phenylalanine and tryptophan.^{32,33} Undigested protein reaches the colon and depending on the microbial composition, transit time, efficiency of host digestion and protein intake, metabolites of protein putrefaction are produced. PAG is known to be a product of protein putrefaction in the colon from

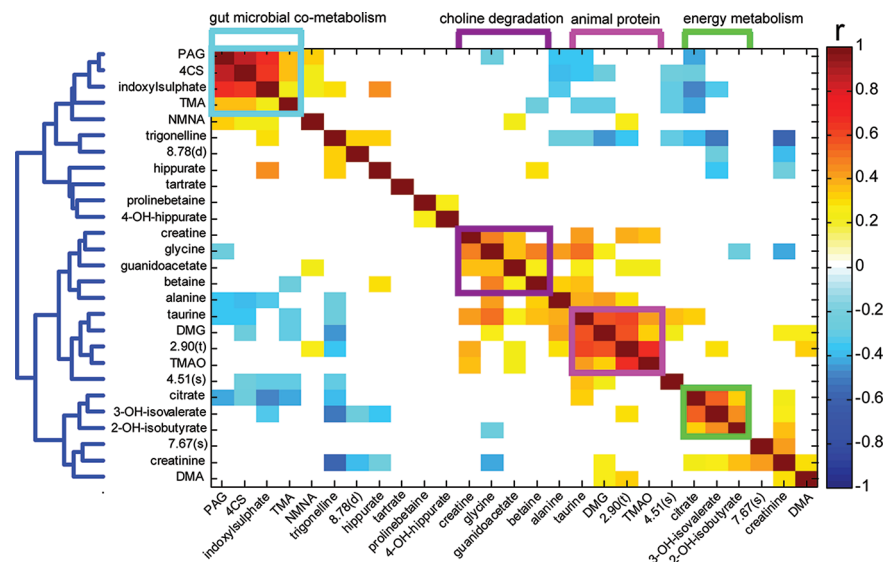


Figure 5. Correlation map calculated using Pearson correlation coefficient highlighting all correlated metabolites with an adjusted p -value < 0.0019 (p -value = 0.05, Bonferroni-corrected for multiple testing). Metabolites were ordered using hierarchical clustering. Color-code: gut microbial-related metabolites (cyan), animal protein-related metabolites (magenta), metabolites from choline degradation (purple), energy metabolism-related metabolites (green).

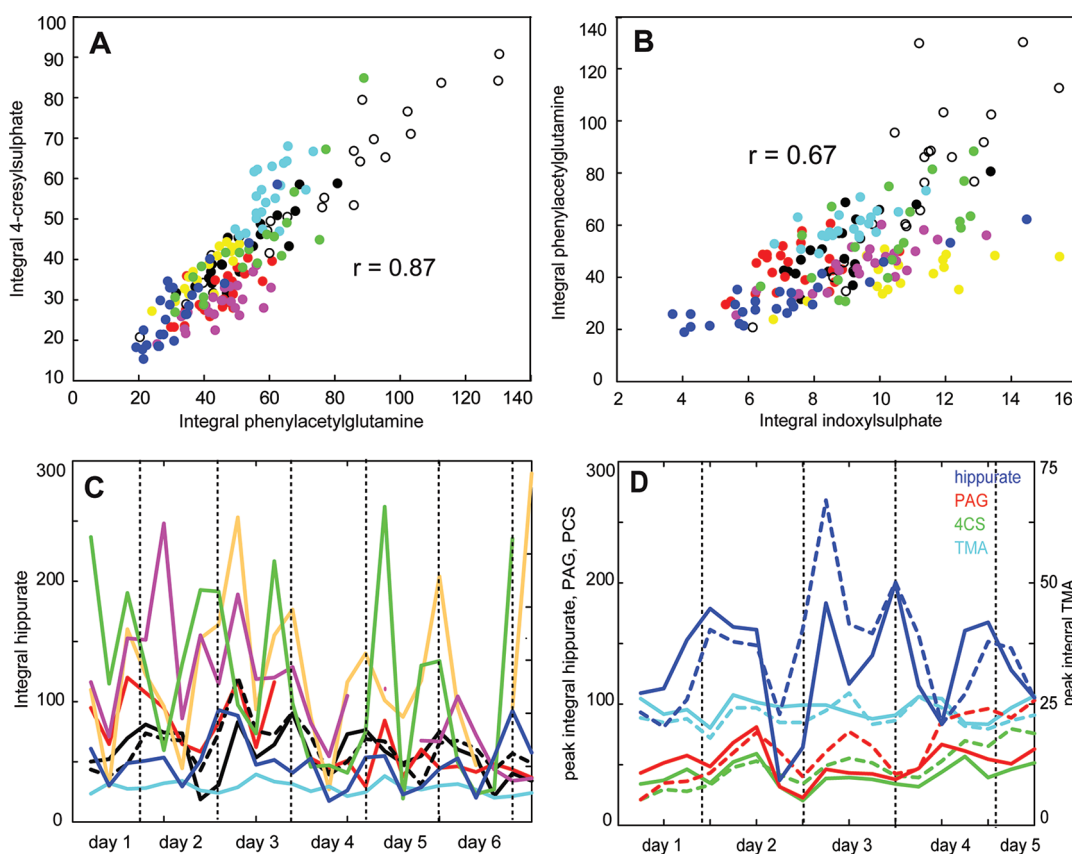


Figure 6. Correlation analysis of (A) phenylacetylglutamine and 4-cresylsulfate and (B) indoxylsulfate and phenylacetylglutamine including data from all volunteers. (C) Peak integral of urinary hippurate over the whole study duration. (Color-code (A)-(C): volunteer 1 (black), volunteer 2 (red), volunteer 3 (blue), volunteer 4 (yellow), volunteer 5 (cyan), volunteer 6 (magenta) and volunteer 7 (green)). (D) Peak integrals of urinary hippurate, PAG, 4CS and TMA from volunteer 1a (solid line) and volunteer 1b (---) plotted over a time course of 18 time points (4,5 days), as a small diet switch occurred on day 6. Both hippurate and TMA correlate very closely between the two study periods. Metabolite quantification derives from integration of normalized NMR spectra.

phenylalanine, where phenylacetate is produced and later conjugated with glutamine in the liver and the gut mucosa.³⁴ 4CS is a

product of microbial tyrosine breakdown via hydroxyphenylacetate to 4-cresol, followed by conjugation with sulfate³⁵ and

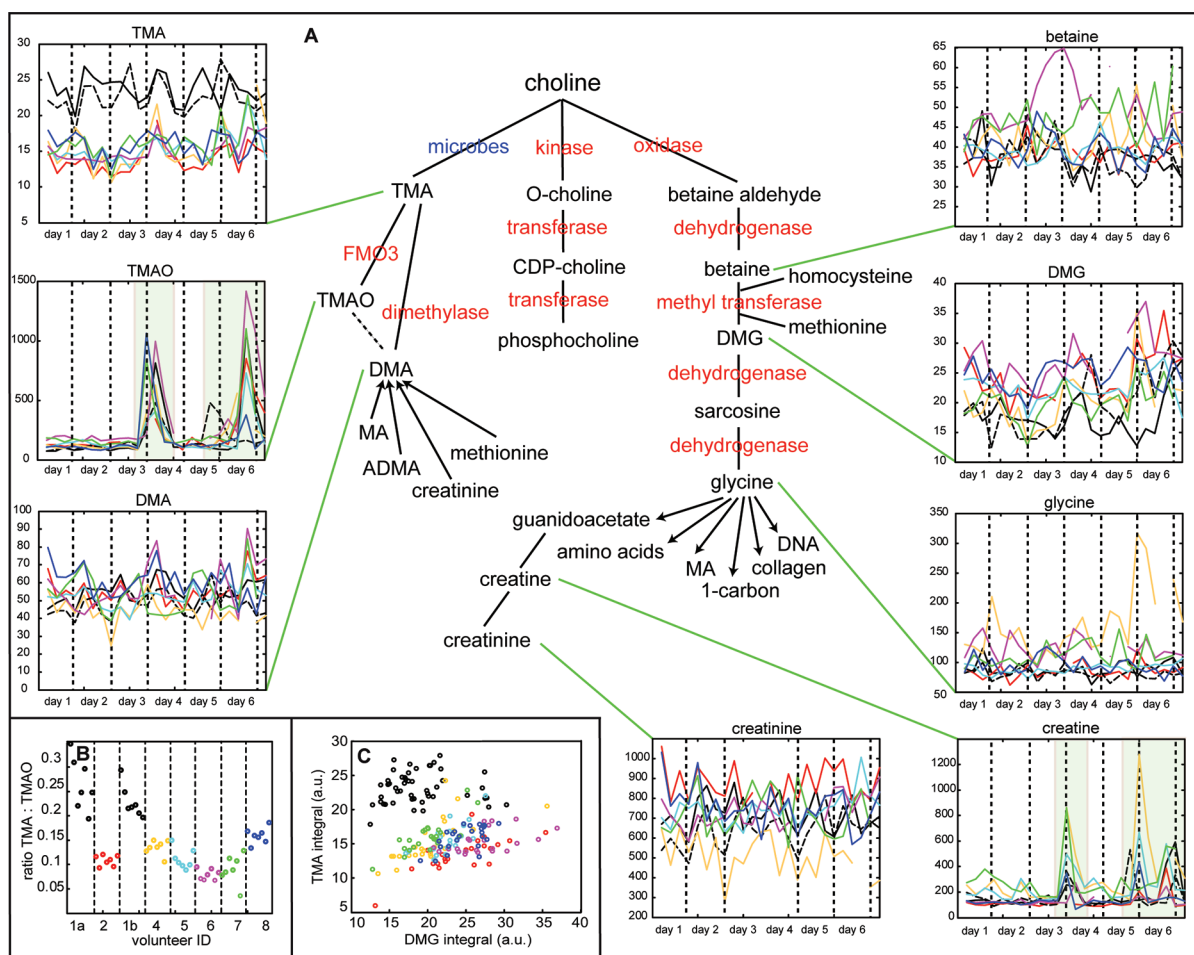


Figure 7. (A) Schematic of the choline degradation pathway, with symbiotic microbial activity highlighted in blue and host enzymes highlighted in red. Dashed arrow represents a putative pathway. Excretion kinetics are shown for every volunteer separately. The time of animal protein consumption is highlighted in green. (B) Ratio of urinary TMA: TMAO of each volunteer, from urine samples prefish or beef consumption. Mean ratios for each individual were: 1a, 0.26; 1b, 0.22; 2, 0.11; 4, 0.13; 5, 0.11; 6, 0.08; 7, 0.10; 8, 0.15. (C) Scatter plot of DMG and TMA (relative concentrations). Color-code of volunteers as follows: volunteer 1, volunteer 2, volunteer 3, volunteer 4, volunteer 5, volunteer 6 and volunteer 7. Metabolite quantification derives from integration of normalized NMR spectra. Abbreviations: MA, methylamine; TMA, trimethylamine; TMAO, trimethylamine-N-oxide; DMG, dimethylglycine; 1-carbon, 1-carbon metabolism.

indoxylsulphate is a product of intestinal tryptophan breakdown and mammalian phase II metabolism.³⁶ Phenylalanine and tyrosine are known to be similarly distributed in the diet with a ratio of 1: 1, while dietary tryptophan sources vary.³⁷

Other markers of microbial activity observed in this study include trimethylamine (TMA), produced from microbial choline degradation (see Figure 6D and 7A), and hippurate, produced from the breakdown of polyphenols and fiber (Figure 6C). Besides the strong correlation of metabolites of protein putrefaction: PAG, 4CS and IS, there was no relationship observed between the choline putrefaction metabolite TMA and the polyphenol breakdown metabolite hippurate. This suggests different microbiota are involved in their production, and/or that they are produced in different sites of the intestine. Indeed, hippurate and TMA³⁸ are known to be mainly produced in the proximal colon, while PAG is produced in the distal colon.³⁹ Hippurate showed high inter-individual as well as intra-individual fluctuations. In particular, volunteer 5 excreted low levels of hippurate in comparison with the other participants, while volunteers 4 and 7 excreted high amounts of hippurate. Dietary

habits are reported to shape the microbiota⁴⁰ and this could be an explanation for the different levels of metabolites between individuals, where, for example, volunteer 5 might not be equipped with a large amount of fiber-digesting bacteria or produces metabolites other than hippurate due to a different microbial composition. This theory could also explain the unassigned resonances (with chemical shifts at δ 2.61 (dd), 2.68 (dd), 5.02 (m), 6.85 (dd), 6.92 (t), 6.99 (d), 7.30 (s), consistent with a 4-hydroxymandelic acid derivate) in the aromatic area for this volunteer, suggesting that volunteer 5 is colonized by bacteria predominantly digesting fiber to aromatic compounds other than (phenyl-)benzoic acid (e.g., phenylacetic acid and phenylcinnamic acid metabolites⁴¹). Further studies combining urinary metabolite profiling and gut microbial community analysis would be helpful to further investigate this hypothesis. The repetition of the diet by volunteer 1 (SI Figure 3, Supporting Information) showed a remarkably stable profile following the dietary challenges, particularly with respect to the ratios of gut microbial metabolites: the integrals of hippurate, PAG, 4CS and TMA were plotted over time to compare changes in these metabolites for the

individual (female, 28 years old, BMI 22 kg/m²) repeating the study after 3 months (Figure 6D). Interestingly, hippurate and TMA correlated closely between the two experiments, suggesting a microbial stability over at least 3 months. Fluctuations of metabolite excretion over at least 18 time points suggest further influence of diet or diurnal effects. Excretion of PAG and 4CS varied between the two experiments with both metabolites increasing over the time course; the ratio of PAG:4CS, however, remained constant.

Specific Investigation of Choline Pathway Metabolites

Consumption of an animal protein meal presents a choline load to each volunteer. The majority of choline gets absorbed and then metabolized to betaine or phosphocholine. Choline remaining in the gut can get fermented to TMA by gut microbes. Two branches will be further investigated here: (i) microbial degradation of choline, generating TMA and further degradation of TMA to TMAO or DMA and (ii) host metabolism of choline to glycine via betaine, DMG and sarcosine, followed by further metabolism to creatine via guanidoacetate and ultimately excretion as creatinine (Figure 7A). Out of the illustrated metabolites, TMAO (end of days 3 and 6) and creatine (end of days 3, 5 and 6) are heavily influenced by ingestion of animal protein, as beef is a good source of creatine and fish is a good source of both TMAO and creatine. TMA shows strong inter-individual variation in overall excretion, with the volunteer repeating the study, volunteer 1a/b, excreting more TMA compared to all other volunteers. Small variations were also introduced by consumption of animal protein, as evidenced by slightly increased urinary TMA levels at the beginning of days 4 and 6 and end of day 6. Further metabolism of TMA to TMAO requires the activity of an enzyme from the flavin-containing monooxygenase (FMO) family, FMO3, which is responsible for oxidation of, for example, nitrogen, phosphorus and sulfur containing compounds.⁴² This enzyme family has been implicated in metabolism of xenobiotics (e.g., drugs and toxins).⁴³ A condition of FMO3 deficiency exists, where patients cannot oxidize TMA and therefore excrete high amounts of TMA, giving urine, sweat and breath a fishy odor, called fish-odor syndrome.^{44,45} These patients can reach a urinary TMA: TMAO ratio of 1.4 while the ratio of healthy subjects is ~0.07.⁴⁶ In this study, the ratio of TMA: TMAO for each volunteer varied between 0.07 and 0.35 (Figure 7 B). Even though volunteer 1 on both diet cycles (a and b) had higher ratios than other participants, it was still considerably lower than that reported in fish-odor syndrome patients.⁴⁶ The gut microbiota-mediated formation of TMA and its further oxidation to TMAO by the host has also been implicated in altering the phenotype of macrophages and hence the promotion of atherosclerotic plaques.⁴⁷

TMAO and DMA excretion were not different in volunteer 1a/1b compared to the other volunteers. Usually, about 20% of urinary DMA comes from TMA.⁴⁸ It can also originate from N-methylation of methylamines derived from glycine and sarcosine, methionine, and the breakdown of creatinine. This latter relationship was illustrated here by a strong correlation of DMA and creatinine ($r = 0.69$). As DMA is involved in other pathways, it is not a candidate biomarker for investigation of choline degradation via gut microbes. About 50% of the absorbed choline is known to be metabolized to betaine in the kidney⁴⁹ and this betaine can be further metabolized to DMG and glycine. Excretion of DMG was reduced in volunteer 1a/1b together with an increased excretion of TMA compared to the other volunteers, as also apparent from looking at the ratio of TMA:DMG

(Figure 7C). In summary, significant inter-individual variability was observed in the choline degradation pathway as exemplified by TMA and DMG excretion.

CONCLUSIONS

Collectively, these data confirm the existence of a personal core metabolic phenotype and highlights several metabolic pathways that are affected by inter-individual differences and differing response to food intake, as well as metabolites that are universally excreted in every volunteer after specific food challenges. Day-to-day variability is strongly coupled to diet for certain metabolites (particularly gut-microbial metabolites), indicating the rapid dynamic response and functional flexibility of the microbiome to changing substrate patterns.^{50,51} The microbial components of the adult human are widely thought to be relatively stable and resistant to diurnal dietary variation. However here we show marked differences in the excretion of gut microbial co-metabolites indicating that the influence of the metagenome is mediated by function rather than composition. These findings underline the importance of conducting clinical trials in a crossover rather than parallel design to have each person act as their own control. On the basis of this, we demonstrated a differential metabolic baseline and suggest a new paradigm for stratification of individuals to implement dietary and drug intervention. These studies emphasize the importance of defining individual metabolite phenotypes for future personalized health care and stratified medicine programs.

ASSOCIATED CONTENT

Supporting Information

Supplementary figures. This material is available free of charge via the Internet at <http://pubs.acs.org>.

AUTHOR INFORMATION

Corresponding Author

*E-mail: j.nicholson@imperial.ac.uk; elaine.holmes@imperial.ac.uk.

REFERENCES

- (1) Gavaghan, C. L.; Holmes, E.; Lenz, E.; Wilson, I. D.; Nicholson, J. K. An NMR-based metabonomic approach to investigate the biochemical consequences of genetic strain differences: application to the C57BL10J and Alpk: ApfCD mouse. *FEBS Lett.* **2000**, *484* (3), 169–174.
- (2) Nicholson, J. K. Global systems biology, personalized medicine and molecular epidemiology. *Mol. Syst. Biol.* **2006**, *2*.
- (3) Holmes, E.; Wilson, I. D.; Nicholson, J. K. Metabolic phenotyping in health and disease. *Cell* **2008**, *134* (5), 714–717.
- (4) WHO, Diet, nutrition and the prevention of chronic diseases - Introduction. In *Diet, Nutrition and the Prevention of Chronic Diseases*; World Health Organization: Geneva, 2003; Vol. 916, pp 1–149.
- (5) Lichtenstein, A. H.; Appel, L. J.; Brands, M.; Carnethon, M.; Daniels, S.; Franch, H. A.; Franklin, B.; Kris-Etherton, P.; Harris, W. S.; Howard, B.; Karanja, N.; Lefevre, M.; Rudel, L.; Sacks, F.; Van Horn, L.; Winston, M.; Wylie-Rosett, J. *Diet and lifestyle recommendations revision 2006 - A scientific statement from the American Heart Association Nutrition Committee* **2006**, *114*, 82. *Circulation* **2006**, *114* (1), 82–96.
- (6) Zeisel, S. H.; Freake, H. C.; Bauman, D. E.; Bier, D. M.; Burrin, D. G.; German, J. B.; Klein, S.; Marquis, G. S.; Milner, J. A.; Pelto, G. H.; Rasmussen, K. M. The nutritional phenotype in the age of metabolomics. *J. Nutr.* **2005**, *135* (7), 1613–1616.
- (7) Lindon, J. C.; Holmes, E.; Bolland, M. E.; Stanley, E. G.; Nicholson, J. K. Metabonomics technologies and their applications in

- physiological monitoring, drug safety assessment and disease diagnosis. *Biomarkers* **2004**, *9* (1), 1–31.
- (8) Kochhar, S.; Jacobs, D. M.; Ramadan, Z.; Berruex, F.; Fuerhox, A.; Fay, L. B. Probing gender-specific metabolism differences in humans by nuclear magnetic resonance-based metabolomics. *Anal. Biochem.* **2006**, *352* (2), 274–281.
- (9) Lenz, E. M.; Bright, J.; Wilson, I. D.; Hughes, A.; Morrisson, J.; Lindberg, H.; Lockton, A. Metabonomics, dietary influences and cultural differences: a 1H NMR-based study of urine samples obtained from healthy British and Swedish subjects. *J. Pharm. Biomed. Anal.* **2004**, *36* (4), 841–849.
- (10) Lenz, E. M.; Bright, J.; Wilson, I. D.; Hughes, A.; Morrisson, J.; Lindberg, H.; Lockton, A. Metabonomics, dietary influences and cultural differences: a H-1 NMR-based study of urine samples obtained from healthy British and Swedish subjects. *J. Pharmaceut. Biomed. Anal.* **2004**, *36* (4), 841–849.
- (11) Wallace, M.; Hashim, Y.; Wingfield, M.; Culliton, M.; McAuliffe, F.; Gibney, M. J.; Brennan, L. Effects of menstrual cycle phase on metabolomic profiles in premenopausal women. *Hum. Reprod.* **2010**, *25* (4), 949–956.
- (12) Bolland, M. E.; Holmes, E.; Lindon, J. C.; Mitchell, S. C.; Branstetter, D.; Zhang, W.; Nicholson, J. K. Investigations into biochemical changes due to diurnal variation and estrus cycle in female rats using high-resolution H-1 NMR spectroscopy of urine and pattern recognition. *Anal. Biochem.* **2001**, *295* (2), 194–202.
- (13) Assfalg, M.; Bertini, I.; Colangiuli, D.; Luchinat, C.; Schafer, H.; Schutz, B.; Spraul, M. Evidence of different metabolic phenotypes in humans. *Proc. Natl. Acad. Sci. U.S.A.* **2008**, *105* (5), 1420–1424.
- (14) Bernini, P.; Bertini, I.; Luchinat, C.; Nepi, S.; Saccetti, E.; Schafer, H.; Schutz, B.; Spraul, M.; Tenori, L. Individual Human Phenotypes in Metabolic Space and Time. *J. Proteome Res.* **2009**, *8* (9), 4264–4271.
- (15) Wang, Y. L.; Tang, H. R.; Nicholson, J. K.; Hylands, P. J.; Sampson, J.; Holmes, E. A metabonomic strategy for the detection of the metabolic effects of chamomile (*Matricaria recutita* L.) ingestion. *J. Agric. Food Chem.* **2005**, *53* (2), 191–196.
- (16) Stella, C.; Beckwith-Hall, B.; Cloarec, O.; Holmes, E.; Lindon, J. C.; Powell, J.; van der Ouderaa, F.; Bingham, S.; Cross, A. J.; Nicholson, J. K. Susceptibility of human metabolic phenotypes to dietary modulation. *J. Proteome Res.* **2006**, *5* (10), 2780–2788.
- (17) Van Dorsten, F. A.; Daykin, C. A.; Mulder, T. P. J.; Van Duynhoven, J. P. M. Metabonomics approach to determine metabolic differences between green tea and black tea consumption. *J. Agric. Food Chem.* **2006**, *54* (18), 6929–6938.
- (18) Walsh, M. C.; Brennan, L.; Malthouse, J. P. G.; Roche, H. M.; Gibney, M. J. Effect of acute dietary standardization on the urinary, plasma, and salivary metabolomic profiles of healthy humans. *Am. J. Clin. Nutr.* **2006**, *84* (3), 531–539.
- (19) Clayton, T. A.; Lindon, J. C.; Cloarec, O.; Antti, H.; Charuel, C.; Hanton, G.; Provost, J. P.; Le Net, J. L.; Baker, D.; Walley, R. J.; Everett, J. R.; Nicholson, J. K. Pharmacometabonomic phenotyping and personalized drug treatment. *Nature* **2006**, *440* (7087), 1073–1077.
- (20) Clayton, T. A.; Baker, D.; Lindon, J. C.; Everett, J. R.; Nicholson, J. K. Pharmacometabonomic identification of a significant host-microbiome metabolic interaction affecting human drug metabolism. *Proc. Natl. Acad. Sci. U.S.A.* **2009**, *106* (34), 14728–14733.
- (21) Winnike, J. H.; Li, Z.; Wright, F. A.; Macdonald, J. M.; O'Connell, T. M.; Watkins, P. B. Use of Pharmaco-Metabonomics for Early Prediction of Acetaminophen-Induced Hepatotoxicity in Humans. *Clin. Pharm. Ther.* **2010**, *88* (1), 45–51.
- (22) Veselkov, K. A.; Lindon, J. C.; Ebbels, T. M. D.; Crockford, D.; Volynkin, V. V.; Holmes, E.; Davies, D. B.; Nicholson, J. K. Recursive Segment-Wise Peak Alignment of Biological H-1 NMR Spectra for Improved Metabolic Biomarker Recovery. *Anal. Chem.* **2009**, *81* (1), 56–66.
- (23) Dieterle, F.; Ross, A.; Schlotterbeck, G.; Senn, H. Probabilistic quotient normalization as robust method to account for dilution of complex biological mixtures. Application in H-1 NMR metabolomics. *Anal. Chem.* **2006**, *78* (13), 4281–4290.
- (24) Blaise, B. J.; Giacometto, J.; Elena, B.; Dumas, M. E.; Toullhoat, P.; Segalat, L.; Emsley, L. Metabotyping of *Caenorhabditis elegans* reveals latent phenotypes. *Proc. Natl. Acad. Sci. U.S.A.* **2007**, *104* (50), 19808–19812.
- (25) Trygg, J.; Wold, S. PLS regression on wavelet compressed NIR spectra. *Chemom. Intell. Lab. Syst.* **1998**, *42* (1–2), 209–220.
- (26) Haydon, G. H.; Jalan, R.; Ala-Korpela, M.; Hiltunen, Y.; Hanley, J.; Jarvis, L. M.; Ludlum, C. A.; Hayes, P. C. Prediction of cirrhosis in patients with chronic hepatitis C infection by artificial neural network analysis of virus and clinical factors. *J. Viral Hepatitis* **1998**, *5* (4), 255–264.
- (27) Vaananen, T.; Koskela, H.; Hiltunen, Y.; Ala-Korpela, M. Application of quantitative artificial neural network analysis to 2D NMR spectra of hydrocarbon mixtures. *J. Chem. Inf. Comput. Sci.* **2002**, *42* (6), 1343–1346.
- (28) Lenz, E. M.; Bright, J.; Wilson, I. D.; Morgan, S. R.; Nash, A. F. P. A H-1 NMR-based metabonomic study of urine and plasma samples obtained from healthy human subjects. *J. Pharm. Biomed. Anal.* **2003**, *33* (5), 1103–1115.
- (29) de Zwart, F. J.; Slow, S.; Payne, R. J.; Lever, M.; George, P. M.; Gerrard, J. A.; Chambers, S. T. Glycine betaine and glycine betaine analogues in common foods. *Food Chem.* **2003**, *83* (2), 197–204.
- (30) Heinzmann, S. S.; Brown, I. J.; Chan, Q.; Bictash, M.; Dumas, M. E.; Kochhar, S.; Stamler, J.; Holmes, E.; Elliott, P.; Nicholson, J. K. Metabolic profiling strategy for discovery of nutritional biomarkers: proline betaine as a marker of citrus consumption. *Am. J. Clin. Nutr.* **2010**, *92* (2), 436–443.
- (31) Chadeau-Hyam, M.; Ebbels, T. M.; Brown, I. J.; Chan, Q.; Stamler, J.; Huang, C. C.; Daviglus, M. L.; Ueshima, H.; Zhao, L.; Holmes, E.; Nicholson, J. K.; Elliott, P.; De Iorio, M. Metabolic profiling and the metabolome-wide association study: significance level for biomarker identification. *J. Proteome Res.* **2010**, *9* (9), 4620–7.
- (32) Power, F. W.; Sherwin, C. P. The detoxification of putrefaction products by the human body. *Arch. Int. Med.* **1927**, *39* (1), 60–66.
- (33) Seakins, J. W. T. Determination of urinary phenylacetylglutamine as phenylacetic acid - studies on its origin in normal subjects and children with cystic fibrosis. *Clin. Chim. Acta* **1971**, *35* (1), 121–131.
- (34) Ramakrishna, B. S.; Gee, D.; Weiss, A.; Pannall, P.; Robertsthomson, I. C.; Roediger, W. E. W. Estimation of phenolic conjugation by colonic mucosa. *J. Clin. Pathol.* **1989**, *42* (6), 620–623.
- (35) Ramakrishna, B. S.; Robertsthomson, I. C.; Pannall, P. R.; Roediger, W. E. W. Impaired sulphation of phenol by the colonic mucosa in quiescent and active ulcerative colitis. *Gut* **1991**, *32* (1), 46–49.
- (36) Elsden, S. R.; Hilton, M. G.; Waller, J. M. End products of metabolism of aromatic amino acids by clostridia. *Arch. Microbiol.* **1976**, *107* (3), 283–288.
- (37) Belitz, H.-D.; Grosch, W.; Schieberle, P.; Burghagen, M. M. *Food Chemistry*; Springer Verlag: Heidelberg, Germany, 2009.
- (38) Zeisel, S. H.; Dacosta, K. A.; Youssef, M.; Hensey, S. Conversion of dietary choline to trimethylamine and dimethylamine in rats - dose-response relationship. *J. Nutr.* **1989**, *119* (5), 800–804.
- (39) Smith, E. A.; Macfarlane, G. T. Enumeration of human colonic bacteria producing phenolic and indolic compounds: Effects of pH, carbohydrate availability and retention time on dissimilatory aromatic amino acid metabolism. *J. Appl. Bacteriol.* **1996**, *81* (3), 288–302.
- (40) De Filippo, C.; Cavalieri, D.; Di Paola, M.; Ramazzotti, M.; Poulet, J. B.; Massart, S.; Collini, S.; Pieraccini, G.; Lionetti, P. Impact of diet in shaping gut microbiota revealed by a comparative study in children from Europe and rural Africa. *Proc. Natl. Acad. Sci. U.S.A.* **2010**, *107* (33), 14691–14696.
- (41) Olthof, M. R.; Hollman, P. C. H.; Buijsman, M.; van Amelsvoort, J. M. M.; Katan, M. B. Chlorogenic acid, quercetin-3-rutinoside and black tea phenols are extensively metabolized in humans. *J. Nutr.* **2003**, *133* (6), 1806–1814.
- (42) Cashman, J. R. Structural and catalytic properties of the mammalian flavin-containing monooxygenase. *Chem. Res. Toxicol.* **1995**, *8* (2), 165–181.
- (43) Lawton, M. P.; Cashman, J. R.; Cresteil, T.; Dolphin, C. T.; Elfarra, A. A.; Hines, R. N.; Hodgson, E.; Kimura, T.; Ozols, J.; Phillips,

I. R.; Philpot, R. M.; Poulsen, L. L.; Rettie, A. E.; Shephard, E. A.; Williams, D. E.; Ziegler, D. M. A nomenclature of the mammalian flavin-containing monooxygenase gene family based on amino acid sequence identities. *Arch. Biochem. Biophys.* **1994**, *308* (1), 254–257.

(44) Ayesh, R.; Mitchell, S. C.; Zhang, A.; Smith, R. L. The fish odor syndrome - biochemical, familial, and clinical aspects. *Br. Med. J.* **1993**, *307* (6905), 655–657.

(45) Mitchell, S. C. The fish-odor syndrome. *Perspect. Biol. Med.* **1996**, *39* (4), 514–526.

(46) Maschke, S.; Wahl, A.; Azaroual, N.; Boulet, O.; Crunelle, V.; Imbenotte, M.; Foulard, M.; Vermeersch, G.; Lhermitte, M. H-1-NMR analysis of trimethylamine in urine for the diagnosis of fish-odour syndrome. *Clin. Chim. Acta* **1997**, *263* (2), 139–146.

(47) Wang, Z. N.; Klipfell, E.; Bennett, B. J.; Koeth, R.; Levison, B. S.; Dugar, B.; Feldstein, A. E.; Britt, E. B.; Fu, X. M.; Chung, Y. M.; Wu, Y. P.; Schauer, P.; Smith, J. D.; Allayee, H.; Tang, W. H. W.; DiDonato, J. A.; Lusis, A. J.; Hazen, S. L. Gut flora metabolism of phosphatidylcholine promotes cardiovascular disease. *Nature* **2011**, *472* (7341), 57–U82.

(48) Zhang, A. Q.; Mitchell, S. C.; Smith, R. L. Dimethylamine in human urine. *Clin. Chim. Acta* **1995**, *233* (1–2), 81–88.

(49) Flower, R. J.; Pollitt, R. J.; Sanford, P. A.; Smyth, D. H. Metabolism and transfer of choline in hamster small intestine. *J. Physiol. (London)* **1972**, *226* (2), 473–489.

(50) Walker, A. W.; Ince, J.; Duncan, S. H.; Webster, L. M.; Holtrop, G.; Ze, X. L.; Brown, D.; Stares, M. D.; Scott, P.; Bergerat, A.; Louis, P.; McIntosh, F.; Johnstone, A. M.; Lobley, G. E.; Parkhill, J.; Flint, H. J. Dominant and diet-responsive groups of bacteria within the human colonic microbiota. *ISME J.* **2011**, *5* (2), 220–230.

(51) Phipps, A. N.; Stewart, J.; Wright, B.; Wilson, I. D. Effect of diet on the urinary excretion of hippuric acid and other dietary-derived aromatics in rat. A complex interaction between diet, gut microflora and substrate specificity. *Xenobiotica* **1998**, *28* (5), 527–37.

(52) van Duynhoven, J.; Vaughan, E. E.; Jacobs, D. M.; Kemperman, R. A.; van Velzen, E. J. J.; Gross, G.; Roger, L. C.; Possemiers, S.; Smilde, A. K.; Dore, J.; Westerhuis, J. A.; Van de Wiele, T. Metabolic fate of polyphenols in the human superorganism. *Proc. Natl. Acad. Sci. U.S.A.* **2011**, *108*, 4531–4538.